

Copper-Activated DNA Photocleavage by a Pyridine-Linked Bis-Acridine Intercalator

María-José Fernández,[†] Beth Wilson,[‡] Marta Palacios,[†] María-Melia Rodrigo,[§] Kathryn B. Grant,^{*,‡} and Antonio Lorente^{*,†}

Departamento de Química Orgánica and Departamento de Química-Física, Universidad de Alcalá, 28871-Alcalá de Henares, Madrid, Spain, and Department of Chemistry, Center for Biotechnology and Drug Design, Georgia State University, P.O. Box 4098, Atlanta, Georgia 30303-4098. Received June 26, 2006; Revised Manuscript Received October 16, 2006

We report the synthesis of new photonuclease **4** consisting of two acridine rings joined by a pyridine-based copper binding linker. We have shown that photocleavage of plasmid DNA is markedly enhanced when this ligand is irradiated in the presence of copper(II) (419 nm, 22 °C, pH 7.0). Viscometric data indicate that **4** binds to DNA by monofunctional intercalation, and equilibrium dialysis provides an estimated binding constant of $1.13 \times 10^5 \text{ M}^{-1}$ for its association with calf thymus DNA. In competition dialysis experiments, **4** exhibits preferential binding to GC-rich DNA sequences. When Cu(II) is added at a ligand to metal ratio of 1:1, electrospray ionization mass spectrometry demonstrates that compound **4** undergoes complex formation, while thermal melting studies show a 10 °C increase in the T_m of calf thymus DNA. Groove binding and intercalation are suggested by viscometric data. Finally, colorimetric and scavenger experiments indicate that the generation of Cu(I), H_2O_2 , and superoxide contributes to the production of DNA strand breaks by the Cu(II) complex of **4**. Whereas the strand breaks are distributed in a relatively uniform fashion over the four DNA bases, subsequent piperidine treatment of the photolysis reactions shows that alkaline labile lesions occur predominantly at guanine.

INTRODUCTION

The design and synthesis of small molecules that bind to and cleave nucleic acids are still major challenges. These artificial nucleases have important applications as tools in molecular biology and as potential therapeutic agents for the treatment of cancer and viral diseases. DNA cleavage is often associated with redox-active or photoactivated transition metal complexes (1–3). To date, a number of metal complexes capable of inducing double-stranded DNA lesions have been developed (4–7).

Photosensitization of intercalating units can promote DNA damage by three main mechanisms: (a) electron transfer from DNA nucleobases, especially guanine, to a photochemically excited state of the intercalator, (b) photogeneration of hydroxyl radicals, an intermediate reactive species which can abstract hydrogen atoms from the DNA sugar backbone, and (c) preferential oxidation of guanines by singlet molecular oxygen generated through energy transfer from an electronically excited photosensitizer (8–11). In some cases, photoreduction of metal complexes is an important step in DNA cleavage reactions (12–16).

Photochemical DNA-cleaving molecules can be used as photonucleases, as photofootprinting agents, and as drugs in photodynamic therapy. Copper exists at micromolar levels in serum and other biological fluids (17) and is closely associated with nucleic acids and chromosomes (18–20), where it is thought to play a role in regulating gene expression (21, 22). Taking this into account, photonucleases which bind to copper may be of greater utility at the cellular level in comparison to photonucleases containing other transition metals or to chemical

nucleases which require an external reducing agent. Accordingly, a number of references on copper binding complexes with photolytic activity have appeared in the literature (14–15, 23–35). While in vivo levels of free copper are tightly controlled by proteins (36–38), the kinetically labile nature of this metal allows ion exchange between small ligands and proteins to take place (38, 39).

Herein, we present the synthesis, characterization, and DNA photocleaving properties of a pyridine-linked bis-acridine intercalator (**4**). We have found that **4** is a good DNA photocleaver, but that cleavage efficiency is markedly enhanced in the presence of Cu(II), converting pUC19 plasmid DNA into its nicked and linear forms upon exposure to visible light (419 nm, pH 7.0, 22 °C). Use of the colorimetric reagent bathocuproinedisulfonic acid disodium salt hydrate (BCS) indicates that the DNA photocleavage reaction involves acridine-sensitized photoreduction of Cu(II) to Cu(I).

MATERIALS AND METHODS

General Procedures. Merck silica gel 60 (230–400 ASTM mesh) was employed for flash column chromatography. TLC was performed on precoated aluminum silica gel plates (Merck or Macherey-Nagel 60F254 0.25 mm). Melting points were determined in an Electrothermal digital IA9100 apparatus. Infrared spectra were taken on an FT-IR Perkin-Elmer 1725X spectrophotometer. All ^1H and ^{13}C NMR spectra were recorded at 300 and 75 MHz, respectively, on a Varian Mercury-VX-300 spectrometer. Chemical shifts are reported in parts per million (ppm) using the residual peaks of either chloroform (δ 7.26 and 77.0 ppm) or methanol (δ 3.30 and 49.0 ppm) as an internal reference. Carbon and proton assignments were based on HSQC and HMBC experiments. CI mass spectra were generated on a Hewlett-Packard HP-5988a spectrometer at 70 eV. An Automass Multi GC/API/MS Finnigan spectrometer was used for ESI mass spectra. Elemental analyses were performed with a Heraeus CHN analyzer. A Cary Bio100 UV–visible

* Corresponding authors. E-mail: antonio.lorente@uah.es; Fax: 34 91 885 46 86 (A.L.). E-mail: kbgrant@gsu.edu; Fax: 1-404-651-1416 (K.B.G.).

[†] Departamento de Química Orgánica, Universidad de Alcalá.

[‡] Georgia State University.

[§] Departamento de Química-Física, Universidad de Alcalá.

spectrophotometer (Varian) was used to plot thermal melting curves, while all other UV–visible spectra were recorded with a Shimadzu UV-1601 or a Lambda 18 Perkin-Elmer spectrophotometer. DNA photolysis reactions were run in an aerobically ventilated Rayonet Photochemical Reactor fitted with eight RPR-4190 Å lamps (The Southern New England Ultraviolet Company).

Reagents were of the highest available purity and were used without further purification. L-Ascorbic acid, catalase, copper(II) chloride dihydrate, sodium phosphate monobasic and dibasic salts, and superoxide dismutase were purchased from Sigma. Glycogen and G-50 Sephadex columns were from Roche Applied Science. Sequenase Version 2.0, Sequenase Stop Solution, and [³⁵S]dATPαS were supplied by Amersham Biosciences. *Eco*RI and *Fsp*I restriction endonucleases were from New England Biolabs. All other chemicals including bathocuproinedisulfonic acid disodium salt hydrate, dimethyl sulfoxide, ethanol, ethidium bromide, D-mannitol, piperidine, and sodium azide were obtained from the Aldrich Chemical Company. Both 2,6-bis[(2-hydroxyethyl)methylaminomethyl]pyridine (**1**) (**40**) and (6-amino-3-acridinyl)carbamic acid methyl ester (**3**) (**41**) were prepared according to reported procedures.

Transformation of *E. coli* competent cells (Stratagene, XL-1 blue) with pUC19 plasmid DNA (Sigma) and growth of bacterial cultures were performed according to established methods (**42**). Purification of the plasmid DNA was accomplished using a Qiagen Plasmid Mega Kit. All enzymes were used according to manufacturer's instructions in the buffers supplied.

2,6-Bis[(2-chloroethyl)methylaminomethyl]pyridine (2). Thionyl chloride (10 mL) was added to 348 mg (1.32 mmol) of 2,6-bis[(2-hydroxyethyl)methylaminomethyl]pyridine (**1**). The reaction mixture was stirred at room temperature for 24 h and then was concentrated at reduced pressure, affording a syrup characterized as **2**·HCl. IR (film): ν 3393, 2968, 2666, 1598, 1463, 1407, 1217, 1160, 756 cm^{-1} . ¹H-NMR (CD₃OD): δ 8.04 (t, J = 7.7 Hz, H4), 7.56 (d, J = 7.7 Hz, 2H, H3, H5), 4.62 and 4.80 (AB, 4H, J = 14 Hz, CH₂-pyr), 4.12 (t, J = 6.4 Hz, 4H, CH₂Cl), 3.69 (m, 4H, CH₂N), 3.01 (s, 6H, CH₃). ¹³C-NMR (CD₃OD): δ 151.44 (C2, C6), 140.92 (C4), 125.41 (C3, C5), 60.54 (CH₂-pyr), 58.33 (CH₂N), 42.21 (CH₃), 38.04 (CH₂Cl). To a solution of 1.23 g (3.08 mmol) of **2**·HCl in methanol (20 mL), 1.14 g (10.78 mmol) of Na₂CO₃ was added. The mixture was stirred for 3 h and then concentrated to dryness. The residue was treated with dichloromethane (25 mL), and the mixture was washed three times with water (10 mL). The organic layer was dried over MgSO₄, filtered, and concentrated at reduced pressure to yield **2** as a brown oil (580 mg, 65%). IR (film): ν 2950, 2795, 1591, 1577, 1455, 1353, 1305, 1262, 1118, 1062, 739 cm^{-1} . ¹H-NMR (CDCl₃): δ 7.65 (t, J = 7.7 Hz, 1H, H4), 7.35 (d, J = 7.7 Hz, 2H, H3, H5), 3.73 (s, 4H, CH₂-pyr), 3.59 (t, J = 6.9 Hz, 4H, CH₂Cl), 2.81 (t, J = 6.9 Hz, 4H, CH₂N), 2.35 (s, 6H, CH₃). ¹³C-NMR (CDCl₃): δ 158.23 (C2, C6), 136.93 (C4), 121.31 (C3, C5), 63.59 (CH₂-pyr), 58.69 (CH₂N), 42.59 (CH₃), 41.56 (CH₂Cl). MS (CI) m/z 290 [M + H]⁺, 39%), 254 (100) (calcd C₁₃H₂₁Cl₂N₃ 289.1). Anal. Calcd for C₁₃H₂₁Cl₂N₃: C, 53.80; H, 7.29; N, 14.48; Cl 24.43. Found: C, 53.94; H, 7.09; N, 14.77.

2,6-Bis{[(6-amino-acridin-3-yl)methoxycarbonylamino]methylaminomethyl}pyridine (4). To a solution of (6-amino-3-acridinyl)carbamic acid methyl ester (**3**) (184 mg, 0.69 mmol) in dry DMF (5 mL), 80% NaH (41 mg, 1.38 mmol) was added. The reaction mixture was stirred under an argon atmosphere for 20 min, and then a solution of 2,6-bis[(2-chloroethyl)methylaminomethyl]pyridine (**2**) (100 mg, 0.345 mmol) in dry DMF (6 mL) was added. The reaction mixture was heated at 50 °C for 20 h, and then concentrated at reduced pressure. The crude product thus obtained was purified by flash

column chromatography on silica gel using ethyl acetate/acetone/triethylamine (5:3:1), affording unreacted carbamate **3**. Continued elution with ethyl acetate/methanol/triethylamine (10:2:1) afforded the desired product as an oil. The product was then dissolved in chloroform and precipitated with diethyl ether, affording 81 mg (31%) of an orange solid. Mp: 128–130 °C. IR (KBr): ν 3414, 1702, 1638, 1612, 1459, 1383, 1158 cm^{-1} . ¹H-NMR (CDCl₃): δ 8.49 (s, 2H, H9), 7.85 (d, J = 2.2 Hz, 2H, H4), 7.80 (d, J = 9.0 Hz, 2H, H1), 7.77 (d, J = 9.0 Hz, 2H, H8), 7.35 (t, J = 7.7 Hz, 1H, H4 pyr), 7.30 (dd, J = 9.0, 2.2 Hz, 2H, H2), 7.19 (d, J = 2.2 Hz, 2H, H5), 7.09 (d, J = 7.7 Hz, 2H, H3, H5 pyr), 7.00 (dd, J = 9.0, 2.2 Hz, 2H, H7), 3.95 (t, J = 6.9 Hz, 4H, CH₂N-acridine), 3.68 (s, 6H, OCH₃), 3.55 (s, 4H, CH₂-pyr), 2.63 (t, J = 6.9 Hz, 4H, CH₂NMe), 2.17 (s, 6H, NCH₃). ¹³C-NMR (CDCl₃): δ 158.40 (C2, C6 pyr), 155.86 (CO), 151.16 (C10a), 149.51 (C4a), 148.65 (C6), 143.57 (C3), 136.57 (C4 pyr), 135.42 (C9), 129.72 (C8), 128.57 (C1), 124.63 (C2), 124.06 (C4), 123.20 (C9a), 121.94 (C8a), 120.82 (C3, C5 pyr), 120.15 (C7), 106.00 (C5), 63.77 (CH₂-pyr), 55.46 (CH₂NMe), 52.96 (OCH₃), 48.31 (CH₂N-acridine), 42.52 (NCH₃). MS (ESI) m/z 752 [M + H]⁺ (calcd for C₄₃H₄₅N₉O₄ 751.36). Anal. Calcd for C₄₃H₄₅N₉O₄: C, 68.69; H, 6.03; N, 16.77. Found: C, 68.81; H, 6.13; N, 16.49. A stock solution of **4** was prepared in dimethyl sulfoxide (purity \geq 99.9%) and was stored at –20 °C until use.

Viscometric Titrations. UltraPure Calf Thymus DNA (Invitrogen Catalog Number 15633–019, average size \leq 2000 bp, 10 mg/mL in ddH₂O) was used without further purification. Viscosity experiments were conducted in a Cannon-Ubbelohde size 75 capillary viscometer immersed in a thermostated, circulating water bath maintained at 25 \pm 0.2 °C. Compound **4** was titrated in buffer A: 6 mM Na₂HPO₄, 2 mM NaH₂PO₄, 1 mM Na₂EDTA, and 15 mM NaCl (pH 7.0). Alternatively, Cu(II) and Cu(II)–**4** (ligand to metal ratio of 1:1) were titrated in buffer B: 20 mM sodium phosphate (pH 7.0). In three separate titrations, a total of five 10- μ L aliquots of each of the following three stock solutions were sequentially added to 1000 μ L of the appropriate buffer in the viscometer containing 200 μ M bp calf thymus (CT) DNA: (i) **4** (400 μ M in buffer A); (ii) Cu(II)–**4** (400 μ M each, in buffer B), and Cu(II) (400 μ M in buffer B). After each sequential addition, the resulting solution was allowed to equilibrate for 15 min before the flow time was recorded with a stopwatch. (The final concentrations of **4**, Cu(II)–**4**, and Cu(II) ranged from 4 to 20 μ M in each of the three titrations.) The flow times of the buffer and then of the DNA in the buffer were also recorded. All measurements were averaged over four trials to an accuracy of \pm 0.2 s. After subtracting the averaged flow time of the buffer, DNA (η_0) and dye-DNA (η) averaged flow times were plotted as (η/η_0)^{1/3} versus the molar ratio r of dye to DNA bp (**43**). Slopes were generated by conducting linear least-square fits to these data (KaleidaGraph version 3.6.4 software).

Competition Dialysis Assay. Calf thymus (CT), *Clostridium perfringens* (CP), and *Micrococcus lysodeikticus* (ML) DNAs and the synthetic polynucleotides poly(dA)–poly(dT), [poly(dGdC)]₂, and [poly(dAdT)]₂ were purchased from Sigma and were used without further purification. A buffer containing 6 mM Na₂HPO₄, 2 mM NaH₂PO₄, 1 mM Na₂EDTA, and 185 mM NaCl (pH 7.0) was utilized in the preparation of all nucleic acid stock solutions. The concentrations of the nucleic acid solutions were determined by UV–visible spectrophotometry using the λ_{max} values and extinction coefficients listed in Table S1 (Supporting Information). In a buffer consisting of 6 mM Na₂HPO₄, 2 mM NaH₂PO₄, 1 mM Na₂EDTA, and 15 mM NaCl (pH 7.0), competition dialysis experiments were performed as described by Chaires (**44**, **45**). For each dialysis assay, a 0.5 mL volume of DNA (75 μ M bp DNA in buffer; Table S1) was

pipetted into one of six individual Spectra/Por DispoDialyzer units (S135062, Spectrum Laboratories, Inc.). The six dialysis units were then placed in a beaker containing 225 mL of a 1.5 μM solution of **4** in buffer. The beaker was covered with Parafilm and wrapped in foil, and its contents were allowed to equilibrate with continuous stirring for 24 h at room temperature (20–22 °C). At the end of the equilibration period, the DNA solutions inside the dialysis units were carefully transferred to microcentrifuge tubes, and a 10.0% (w/v) stock solution of sodium dodecyl sulfate (SDS) was added to give a final concentration of 1.0% (w/v). The DNA–SDS solutions were allowed to equilibrate for 2 h, after which the total concentration of ligand **4** (C_t) was determined by UV–visible absorbance measurements using the extinction coefficient for free ligand **4** in the presence of 1.0% SDS ($\epsilon_{451} = 22\,716\text{ M}^{-1}\text{ cm}^{-1}$). An appropriate correction for the slight dilution of the sample resulting from the addition of SDS stock solution was made. The concentration of free ligand **4** (C_f ; $\epsilon_{451} = 12\,500\text{ M}^{-1}\text{ cm}^{-1}$) was also determined spectrophotometrically using an aliquot of the dialysate solution. The amount of DNA-bound **4** (C_b) was calculated by the difference ($C_b = C_t - C_f$).

Thermal Melting Studies. Individual 3 mL solutions containing 15 μM bp of calf thymus DNA (Invitrogen cat. #15633–019) in 20 mM sodium phosphate buffer pH 7.0 or in 20 mM sodium phosphate buffer pH 7.0, 10 μM **4**, and/or 10 μM CuCl_2 were placed in 3 mL (1 cm) quartz cuvettes (Starna). The DNA was then denatured by increasing the temperature from 25 °C to 100 °C at a rate of 0.5 °C min^{-1} , while absorbance was monitored at 260 nm. *KaleidaGraph* version 3.5 software was used to approximate the first derivative of $\Delta A_{260}/\Delta T$ vs temperature, where the T_m value for each melting transition was marked by the maximum of the first derivative plot.

Photocleavage of Supercoiled Plasmid DNA. Concentration profile reactions were conducted in a volume of 20 μL as follows. A total of 38 μM bp of pUC19 plasmid DNA in 20 mM sodium phosphate buffer pH 7.0 or in 20 mM sodium phosphate buffer pH 7.0, 50 μM , 30 μM , 20 μM , 10 μM , 5 μM , or 2 μM of CuCl_2 and/or 1 mol equiv (50 μM , 30 μM , 20 μM , 10 μM , 5 μM , or 2 μM) of **4** was irradiated for 50 min at 419 nm and 22 °C. A parallel control reaction consisting of 20 mM sodium phosphate buffer pH 7.0, 38 μM bp of pUC19, 50 μM of CuCl_2 , and 50 μM of **4** was kept in the dark for 50 min.

Individual time course reactions were conducted in a volume of 20 μL . A total of 38 μM bp of pUC19 plasmid DNA in 20 mM sodium phosphate buffer pH 7.0 or in 20 mM sodium phosphate buffer pH 7.0, 50 μM CuCl_2 , and/or 50 μM **4** was irradiated at 419 nm and 22 °C. The 20 μL reactions were removed from the Rayonet Photochemical Reactor at 10, 20, 30, 40, or 50 min time intervals. Parallel controls consisting of 20 mM sodium phosphate buffer pH 7.0, 38 μM bp of pUC19 plasmid, 50 μM of CuCl_2 , and/or 50 μM of **4** were kept in the dark for 50 min.

After the addition of 3 μL of electrophoresis loading buffer to the photocleavage reactions (15.0% (w/v) Ficoll, 0.025% (w/v) bromophenol blue), cleavage products were separated on a 1.0% nondenaturing agarose gel stained with ethidium bromide (0.5 $\mu\text{g}/\text{mL}$). To determine the percent conversion of supercoiled plasmid DNA to nicked and linear forms, the gel was visualized on a transilluminator set at 302 nm, photographed, and then quantitated using *ImageQuant* v. 5.2 software (Amersham Biosciences).

Colorimetric Detection of Copper(II). A series of 500 μL reactions was prepared in which each contained 20 mM sodium phosphate buffer pH 7.0 and one or more of the following reagents: 50 μM of **4**, 50 μM of CuCl_2 , and 38 μM bp of pUC19 plasmid DNA. The samples were irradiated at 419 nm in the absence and presence of 100 μM of bathocuproinedisulfonic

acid disodium salt hydrate, while a parallel set of reactions was kept in the dark. After 50 min, the solutions were visually examined for color change, placed in 500 μL quartz cuvettes, and monitored between 200 and 600 nm for evidence of Cu(II) –bathocuproine complex formation. As a positive control, 500 μL samples containing 20 mM sodium phosphate buffer pH 7.0 and 100 μM bathocuproinedisulfonic acid disodium salt hydrate in the presence of 50 μM CuCl_2 or 50 μM CuCl_2 and 50 μM L-ascorbic acid were reacted at 22 °C for 1 min, after which, UV–visible spectra were recorded.

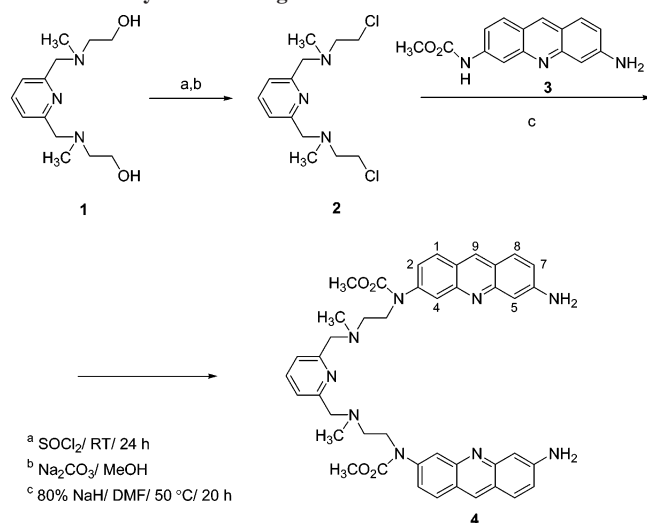
Inhibition of DNA Photocleavage. Twenty microliter reactions containing 20 mM sodium phosphate buffer pH 7.0, 38 μM bp pUC19 plasmid DNA, 50 μM of **4**, and 50 μM of CuCl_2 were irradiated at 419 nm for 50 min in the presence of either 100 mM sodium azide, 100 mM D-mannitol, 100 U superoxide dismutase, 100 U catalase, or 100 μM bathocuproinedisulfonic acid disodium salt hydrate. Reaction products were then resolved on a 1.0% nondenaturing agarose gel and quantitated as described above. The percent inhibition of DNA photocleavage was calculated on the basis of a comparison to parallel reactions run in the absence of scavenger or chelator.

DNA Photocleavage at Nucleotide Resolution. *EcoRI* linearized pUC19 plasmid was 3'-end-labeled using *Sequenase* version 2.0 and [^{35}S]dATP α S according to an established laboratory protocol (46). Unincorporated nucleotides were removed with a G-50 Sephadex spun column. The DNA was then digested with *FspI* to produce a restriction fragment 138 bp in length and resolved on a 2.0% agarose gel. The fragment was excised, and DNA was isolated using a QIAquick Gel Extraction Kit purchased from Qiagen. The purified DNA was stored in a total volume of 400 μL of deionized, distilled water at –78 °C.

Typical photocleavage reactions contained 15 μM bp of the 138 bp DNA fragment in 20 mM sodium phosphate buffer pH 7.0 or in 20 mM sodium phosphate buffer pH 7.0, 5 μM **4** and 5 μM CuCl_2 (50 μL total volume). The samples were irradiated for 2 h at 419 nm, after which, DNA was precipitated with 40 μg glycogen/2.5 volumes EtOH, and washed with 70.0% EtOH. A duplicate set of reactions was precipitated, dissolved in 100 μL of 1.0% piperidine, heated at 90 °C for 30 min, and then lyophilized to dryness. Cleavage products without and with piperidine treatment were dissolved in 4 μL of *Sequenase* Stop Solution (95.0% (v/v) deionized formamide, 10 mM EDTA, 0.1% (w/v) xylene cyanol and 0.1% (w/v) bromophenol blue), denatured for 3 min at 95 °C, and resolved on a 10.0% denaturing polyacrylamide gel adjacent to G, G + A, and T chemical sequencing reactions. To determine yields, the gel was scanned with a *FujiFilm Image Reader* v. 2.01 Gel Imaging System. The resulting storage-phosphor autoradiogram was quantitated using *FujiFilm ImageGauge* v. 3.41 software. The DNA sequencing reactions were performed as previously described (46).

RESULTS AND DISCUSSION

Our approach to the design of ligand **4** combines a 2,6-bis-(aminomethyl)pyridine-based copper binding moiety and two photochemically active 3,6-acridinediamine groups as DNA recognition elements. The ligand 2,6-bis-(aminomethyl)pyridine and its amino-*N*-substituted analogs form stable 1:1 complexes with Cu(II) ($\log Q_{\text{Cu(II)}} = 15.2\text{--}15.7$, equilibrium quotient $Q = [\text{ML}]/[\text{M}][\text{L}]$; refs 47 and 48). Alternatively, acridine orange, proflavin, and other 3,6-acridinediamines intercalate into DNA and, upon irradiation with visible light, efficiently effect DNA photocleavage (16, 49–51). Therefore, the acridine rings of **4** were intended to increase DNA binding and to initiate DNA photocleavage. We also took into account that cleavage levels might be enhanced by acridine-sensitized photoreduction of pyridine-bound copper(II).

Scheme 1. Synthesis of Ligand 4

Synthesis of Ligand 4. Compound **4** was obtained from 2,6-bis[(2-hydroxyethyl)methylaminomethyl]pyridine (**1**) (*40*), which upon treatment with thionyl chloride at room temperature for 24 h, followed by basification with sodium carbonate, afforded 2,6-bis[(2-chloroethyl)methylaminomethyl]pyridine (**2**) as a brown oil in 65% yield. Compound **2** was reacted with (6-amino-3-acridinyl)carbamic acid methyl ester (**3**) (*41*) in anhydrous DMF with 80% NaH as base at 50 °C for 20 h (Scheme 1). Purification of the crude product afforded **4** in 31% yield.

Viscometric Analysis. In order to test for the intercalating ability of **4** and to further examine its behavior as a groove binder or as a mono- or bis-intercalator, DNA viscosity measurements were conducted. In the process of intercalation, helical DNA unwinds to accommodate planar aromatic ring systems that become inserted in between DNA base pairs. This process is accompanied by an effective increase in contour length that adds to the intrinsic viscosity of the DNA polymer. Because groove binding compounds do not markedly lengthen helical DNA, there is no significant change in viscosity (*52*). Consequently, viscometric titrations represent a highly reliable method for establishing the binding modes of DNA interacting ligands (*52*).

The viscometry data for compound **4** and copper(II) are presented as plots of $(\eta/\eta_0)^{1/3}$ versus r (the molar ratio of added compound to DNA base pairs) according to the theory of Cohen and Eisenberg (*43*). Figure 1 shows that compound **4** increases the relative viscosity of calf thymus DNA as a function of increasing r and that the slope (0.82) obtained from the $(\eta/\eta_0)^{1/3}$ versus r plot falls within the range expected for mono-functional intercalators (*53*). It is conceivable that the lowest-energy conformation of **4** is incompatible with the neighbor exclusion principle and therefore permits the intercalation of only one acridine ring. In contrast, the viscometric data of copper(II) with CT DNA yield slopes of -0.12 and 0.41 in the absence and presence of 1 mol equiv of **4**, respectively. The observed reduction in slope from 0.82 to 0.41 may indicate that interaction of the compound's 2,6-bis(aminomethyl)pyridine linker with copper(II) induces a conformational change that introduces a competing, non-intercalative DNA binding mode, most likely groove binding. Notwithstanding, the increase in the apparent DNA contour length by the copper(II) complex of **4** is still substantial, suggesting some degree of intercalative binding (*54*).

Electrospray Ionization Mass Spectrometry. Our next goal was to obtain direct evidence of copper(II) complex formation. Ligand **4** was reacted with CuCl₂ in HPLC-grade methanol at

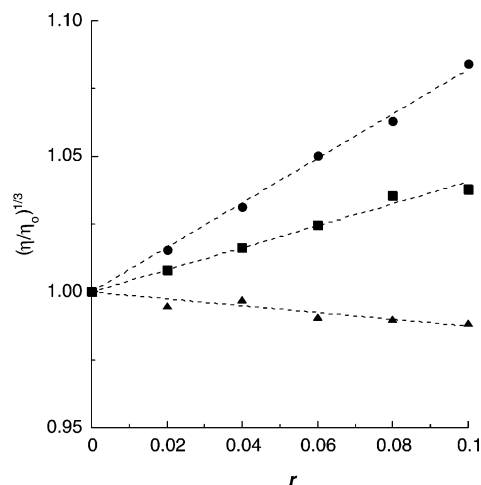


Figure 1. Change in relative viscosity $(\eta/\eta_0)^{1/3}$ of CT DNA as a function of r , the molar ratio of compound to DNA base pairs. Viscometric titrations were conducted in the presence of (i) compound **4** (●; slope = 0.82; 6 mM Na₂HPO₄, 2 mM NaH₂PO₄, 1 mM Na₂EDTA, and 15 mM NaCl buffer pH 7.0); (ii) compound **4** and copper(II) at a ligand to metal ratio of 1:1 (■; slope = 0.41; 20 mM sodium phosphate buffer pH 7.0); (iii) copper(II) (▲; slope = -0.12 ; 20 mM sodium phosphate buffer pH 7.0).

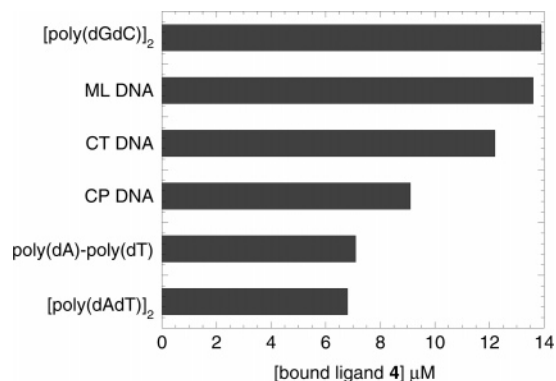


Figure 2. The bar graph indicates the concentrations of DNA-bound ligand **4** detected after a 24 h equilibration in competition binding dialysis studies of six DNA sequences.

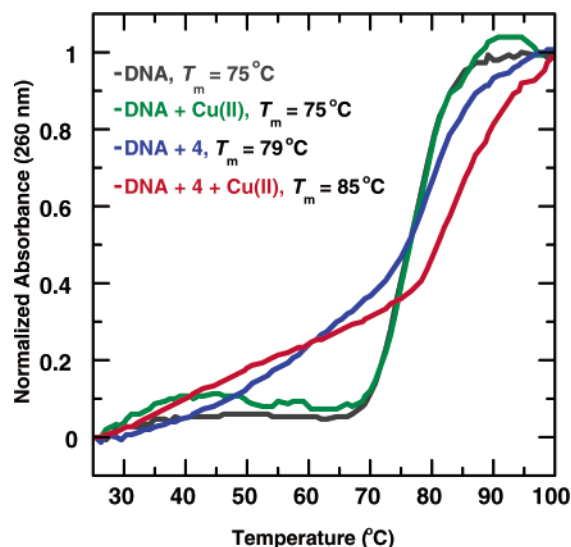
a ligand to metal ratio of 1:1 (90 min, 22 °C), after which a positive-ion electrospray (ESI) mass spectrum was recorded (Figure S1 in Supporting Information). Isotopic distributions of molecular ions corresponding to the following 1:1 metallic complexes were observed: (i) [4HCuCl]²⁺ between 425 and 428 m/z (calcd for [C₄₃H₄₆N₉O₄CuCl]²⁺ 425.13); (ii) [4CuCl]¹⁺ between 849 and 855 m/z (calcd for [C₄₃H₄₅N₉O₄CuCl]¹⁺ 849.26); and (iii) [4HCuCl₂]¹⁺ between 885 and 892 m/z (calcd for [C₄₃H₄₆N₉O₄CuCl₂]¹⁺ 885.24).

Competition Dialysis. The results of dialysis experiments are depicted in a bar graph which shows the concentrations of ligand **4** bound to calf thymus, *Clostridium perfringens*, and *Micrococcus lysodeikticus* DNAs and to the synthetic, double-helical polynucleotides poly(dA)-poly(dT), [poly(dGdC)]₂, and [poly(dAdT)]₂ (Table S1, Figure 2). The data were obtained after equilibrating 1.5 μM of **4** (in the dialysate solution) and 75 μM bp of nucleic acid (in each sample dialysis unit) for 24 h. At the end of the equilibration period, UV-visible spectra were recorded in order to determine the concentrations of free ligand **4** and DNA-bound **4**. The amount of the DNA-bound ligand was averaged over three trials, and the estimated error was between 5% and 10% for each nucleic acid structure tested. The competition dialysis data were then used to calculate the apparent association constants of ligand **4**, given by $K_{app} = C_b/C_f$ [DNA], where C_b and C_f are the DNA-bound and free ligand

Table 1. Apparent Association Constants Obtained by Competition Dialysis^a

deoxyribonucleic acid	$K_{app} \times 10^5 \text{ M}^{-1}$
[poly(dGdC)] ₂ (100% GC)	1.30
ML DNA (72% GC)	1.26
CT DNA (42% GC)	1.13
CP DNA (31% GC)	0.85
poly(dA)-poly(dT) (0% GC)	0.66
[poly(dAdT)] ₂ (0% GC)	0.63

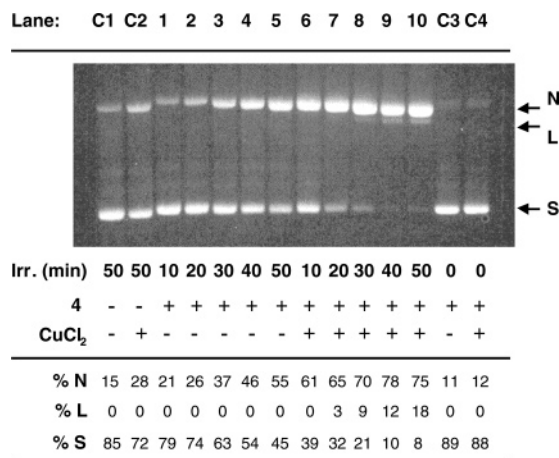
^a The abbreviations ML DNA, CT DNA, and CP DNA correspond to *Micrococcus lysodeikticus*, calf thymus, and *Clostridium perfringens* DNAs, respectively.

**Figure 3.** Thermal melting curves and T_m values of 15 μM bp calf thymus DNA in the absence and presence of 10 μM **4** and/or 10 μM CuCl_2 (20 mM sodium phosphate buffer pH 7.0).

concentrations, respectively, and [DNA] is the concentration of DNA in molar base pairs (Table 1).¹ Clearly, the data in Figure 2 and Table 1 indicate that ligand **4** shows a preference for GC base pairs as exemplified by an increase in levels of binding to ML DNA (71% GC, $K_{app} = 1.26 \times 10^5 \text{ M}^{-1}$) relative to CP DNA (31% GC; $K_{app} = 0.85 \times 10^5 \text{ M}^{-1}$).

Thermal Melting Studies. The majority of DNA intercalators bind to double-helical DNA through a combination of π - π stacking and electrostatic interactions. As a consequence, double-helical DNA is stabilized, and the melting temperature (T_m) of the duplex is increased as a function of the increasing binding affinity of the intercalator (55). Melting temperature (T_m) values of 15 μM bp calf thymus DNA in 20 mM sodium phosphate buffer pH 7.0 were derived from thermal melting curves recorded at 260 nm (Figure 3). While 10 μM of Cu(II) had no effect in the absence of the ligand, 10 μM of **4** increased the T_m of calf thymus DNA by 4 °C and 10 °C in the absence and presence of 10 μM concentrations of Cu(II) , respectively. Taken together, these data indicate that **4** binds to double-helical DNA, thereby increasing its stability. Duplex stability is then further enhanced by the interaction of **4** with copper(II). In light of the above viscometric data, this result would appear to suggest that groove binding and intercalation of **4** in the presence of Cu(II) might stabilize duplex DNA to a greater degree than

¹ Competition dialysis experiments were conducted at room temperature in sodium phosphate buffer pH 7.0. Under these conditions, the UV-vis spectra of the Cu(II) complex of **4** and of ligand **4** were found to be nearly superimposable. Therefore, the K_{app} of the Cu(II) complex of **4** could not be accurately determined by competition dialysis because the concentration of the Cu(II) complex of **4** versus that of **4** could not be ascertained.

**Figure 4.** A photograph of a 1.0% nondenaturing agarose gel showing photocleavage of pUC19 plasmid DNA in the presence of 50 μM of **4** without and with 50 μM of CuCl_2 (22 °C, pH 7.0). C1 and C2 correspond to DNA irradiated at 419 nm, without and with CuCl_2 , respectively (no **4**). C3 and C4 correspond to DNA treated for 50 min with **4**, without and with CuCl_2 , respectively (no $h\nu$). Lanes 1–10 correspond to DNA irradiated at 419 nm for 10, 20, 30, 40, and 50 min in the presence of **4**, without and with CuCl_2 . The above yields corresponding to C1, C2, Lane 5, and Lane 10 were averaged over three trials with standard deviations of $\pm 3\%$, $\pm 5\%$, $\pm 3\%$, and $\pm 2\%$, respectively. S, L, and N designate supercoiled, linear, and nicked forms of pUC19 plasmid DNA.

simple monointercalation. It is also conceivable that complex formation with positively charged copper might enhance electrostatic interactions between **4** and the negatively charged phosphate backbone of the DNA duplex. Notwithstanding, the increase in T_m observed when Cu(II) is added to **4** indicates that the apparent DNA association constant K_{app} of the Cu(II) complex of **4** is higher than the K_{app} of the free ligand **4**.¹ The small increases in low-temperature absorbance produced by compound **4** and its Cu(II) complex probably arise from thermally induced changes in the ratio of DNA-bound ligand to free ligand (Figure 3; ref 56).

Photocleavage of Supercoiled Plasmid DNA. To detect the formation of DNA frank strand breaks,² a preliminary concentration profile was conducted in which individual samples containing 38 μM bp of pUC19 plasmid DNA in 20 mM sodium phosphate buffer pH 7.0 were equilibrated with 50 μM to 2 μM of **4** in the absence and presence of 1 mol equiv of CuCl_2 . The samples were irradiated for 50 min at 419 nm and 22 °C in an aerobically ventilated Rayonet Photochemical Reactor, after which, DNA photocleavage products were resolved on a 1.0% nondenaturing agarose gel. The results of the profile showed that 1 mol equiv of Cu(II) enhanced DNA photocleavage produced by 50 to 20 μM concentrations of compound **4** in a concentration-dependent fashion, with maximum levels of photocleavage occurring in the 50 μM reaction (Figure S2 in Supporting Information).

DNA photocleavage as a function of time was studied next. Reactions consisting of 20 mM sodium phosphate buffer pH 7.0 with 38 μM bp pUC19 plasmid DNA, 50 μM of compound **4**, and 50 μM of CuCl_2 were irradiated as described above, except that the reactions were removed at 10 to 50 min time points prior to agarose gel electrophoresis. While 50 μM of intercalator **4** clearly demonstrated time-dependent DNA photocleavage (Figure 4, lanes 1 to 5), reaction yields were markedly enhanced at all time points upon the addition of

² DNA frank strand breaks are defined as single- or double-stranded DNA breaks directly induced by the effects of a cleaving reagent, in the absence of subsequent treatment with alkaline or with a secondary amine such as piperidine.

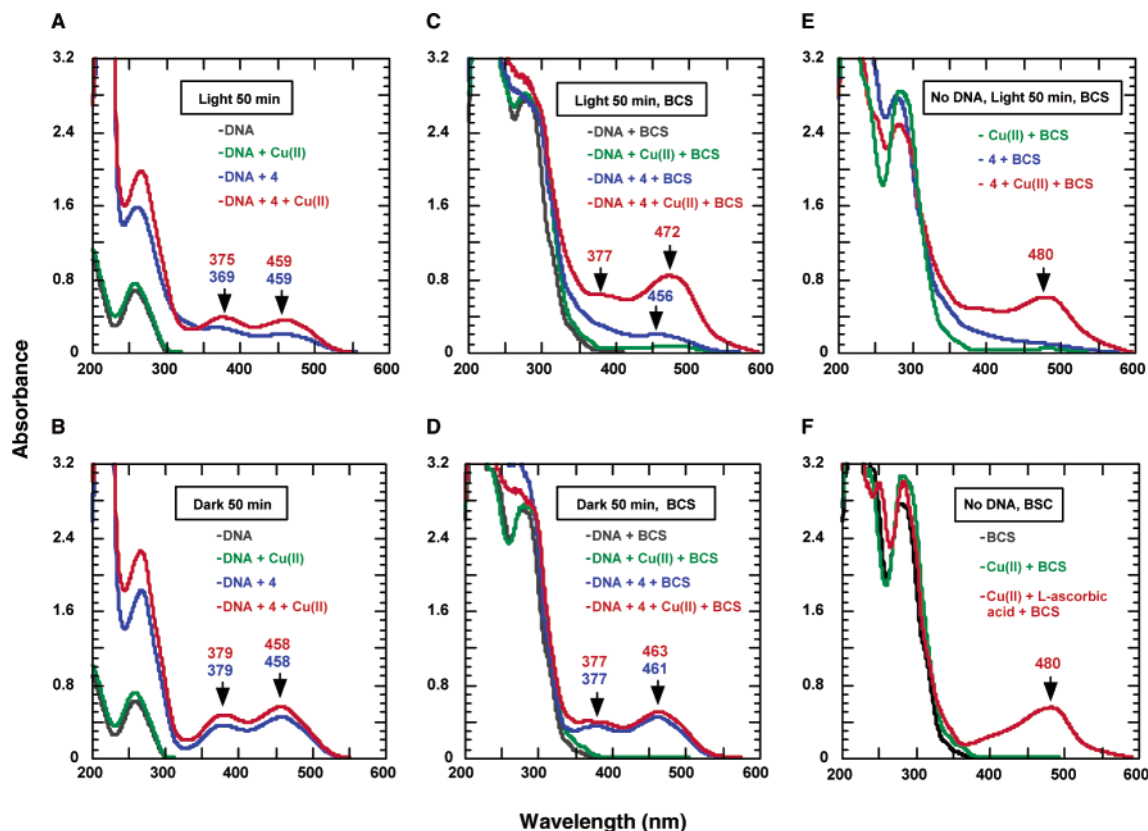


Figure 5. UV–visible spectra to assay for Cu(I)-BCS complex formation in 20 mM sodium phosphate buffer pH 7.0, 22 °C.

equivalent concentrations of CuCl_2 (Figure 4, lanes 6 to 10). (Virtually no cleavage was observed in parallel control reactions run in the dark; Figure 4, lanes C3 and C4.) Notably, after 50 min of irradiation, supercoiled plasmid was converted into 28% nicked DNA in the presence of Cu(II)/buffer , 55% nicked in **4**/buffer, and 75% nicked plus 18% linear when **4**/ Cu(II)/buffer were present in combination (Figure 4, lanes C2, 5, and 10, respectively). Taking into consideration that 15% of photonic DNA was produced in buffer alone, it is evident that ligand **4** and Cu(II) interact in a synergistic rather than additive fashion. Because photoreduction of Fe(III) is readily effected with visible light by means of electron transfer from the photochemically excited triplet states of acridine orange and other 3,6-diamino-acridines (57, 58), we hypothesized that a potential source of synergism might involve acridine-sensitized photoreduction of pyridine-bound Cu(II) . Subsequent reaction of Cu(I) with O_2 would be expected to generate DNA cleaving, reactive oxygen species (59–61).

Colorimetric Detection of Copper(I). Our next goal was to obtain experimental evidence that would substantiate photoreduction of Cu(II) by ligand **4**. We utilized a colorimetric assay based on bathocuproinedisulfonic acid disodium salt hydrate (BCS), which forms a 2:1 stable, brightly colored orange complex with Cu(I) ($\lambda_{\text{max}} = 480 \text{ nm}$; $\epsilon = 13\,500 \text{ M}^{-1} \text{ cm}^{-1}$; ref 62). Photolysis reactions in 20 mM sodium phosphate buffer pH 7.0 were irradiated at 419 nm and 22 °C for 50 min in the presence of one or more of the following reagents: 50 μM **4**, 50 μM CuCl_2 , 38 μM bp pUC19 plasmid DNA, and 100 μM BCS; after which UV–visible spectra were immediately recorded (Figure 5). Parallel reactions run in the dark were used as negative controls (Figure 5B,D). As a control for BCS– Cu(I) complex formation, 100 μM BCS was reacted with 50 μM CuCl_2 in the absence and presence of 50 μM of the reducing agent L-ascorbic acid (Figure 5F).

As expected, the addition of BCS to Cu(II) produced a bright orange color and signature 480 nm absorption in the L-ascorbic

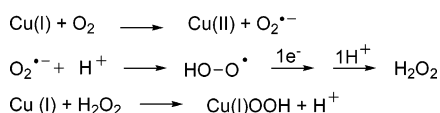
acid control reaction (Figure 5F), but not in any of the dark DNA reactions (even those containing **4** and/or Cu(II) ; Figure 5B,D), and not in any reactions in which BCS was omitted (Figure 5A,B). However, the DNA reaction irradiated in the presence of ligand **4**, Cu(II) , and BCS produced a significant orange color change. In addition, a strong hyperchromic absorption band indicative of the formation of a BCS– Cu(I) complex was observed at 472 nm (Figure 5C: DNA + **4** + Cu(II) + BCS). (Spectral overlap with **4** and/or one of its photoproducts most likely accounts for the 8-nm blue shift relative to 480 nm: Figure 5C compared to Figure 5E,F.) Importantly, there was no evidence of BCS– Cu(I) complex formation when **4** was omitted from the photocleavage reaction (Figure 5C: DNA + Cu(II) + BCS). When DNA was left out, significant absorption and color were still produced (Figure 5E: **4** + Cu(II) + BCS). Therefore, the BCS data collectively indicate that bis-acridine ligand **4** sensitizes photoreduction of Cu(II) to Cu(I) and that DNA is not required for photoreduction.

Inhibition of DNA Photocleavage. To further investigate mechanism(s) underlying the Cu(II) -assisted formation of DNA frank strand breaks, we conducted the following inhibition experiments. Individual photocleavage reactions consisted of 38 μM bp of pUC19 plasmid DNA, 50 μM of **4**, and 50 μM of CuCl_2 pre-equilibrated with one of the following reagents: the singlet oxygen ($^1\text{O}_2$) scavenger sodium azide, the hydroxyl radical ($\bullet\text{OH}$) scavenger D-mannitol, the hydrogen peroxide (H_2O_2) scavenger catalase, the superoxide ($\text{O}_2^{\bullet-}$) scavenger superoxide dismutase (SOD), and the Cu(I) -specific chelating agent BCS. From examination of the data in Table 2, it is evident that sodium azide, catalase, and BCS blocked frank strand break formation to a significant degree, while D-mannitol was almost completely ineffective. Intermediate levels of inhibition were produced by SOD, indicating that superoxide contributes to photocleavage. (SOD produces H_2O_2 , which can itself play a part in cleavage and thereby lower inhibition by this enzyme.) Although the piperidine-labile lesion 8-hydroxyguanosine is the

Table 2. Average % Inhibition of DNA Photocleavage by Scavengers and BCS^a

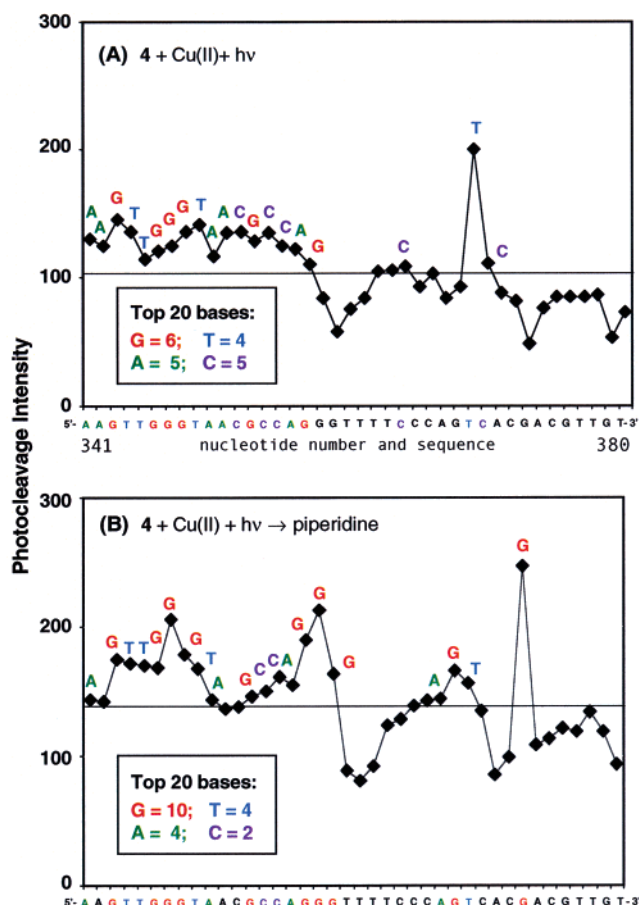
scavenger/chelator	species targeted	percent inhibition
D-mannitol (100 mM)	•OH	5 ± 1
superoxide dismutase (100 U)	O ₂ • ⁻	29 ± 1
(BCS 100 μM)	Cu(I)	51 ± 2 ^b
catalase (100 U)	H ₂ O ₂	56 ± 2
sodium azide (100 mM)	¹ O ₂	61 ± 3

^a Individual reactions consisting of 38 μM bp of pUC19 plasmid DNA equilibrated with 50 μM of **4** and 50 μM of CuCl₂, and one of the above reagents were irradiated under aerobic conditions at 419 nm for 50 min at 22 °C. Percent inhibition was averaged over three trials with error reported as standard deviation. Final reagent concentrations are in parenthesis. ^b In control experiments, we observed direct photocleavage of DNA by BCS in the absence of **4** (data not shown). Therefore, the 51% inhibition produced by BCS may be lower than the actual % inhibition value.

**Figure 6.** A proposed model in which superoxide (O₂•⁻), hydrogen peroxide (H₂O₂), and Cu(I) contribute to the formation of a Cu(I)-peroxide complex.

primary form of DNA damage produced by singlet oxygen, the relative efficiency of sodium azide implies that singlet oxygen may play a major role: singlet oxygen is capable of cleaving DNA directly by producing frank strand breaks at guanine bases (63). However, because frank strand breaks account for no more than 5% of total DNA damage produced by ¹O₂ (64), it is conceivable that cleavage inhibition by sodium azide involves a copper–peroxide-type complex (60) of ligand **4**. The relatively strongly inhibitory effects of catalase and of the Cu(I)-specific chelating agent BCS clearly indicate that hydrogen peroxide and Cu(I) participate in DNA photocleavage. Alternatively, the ineffectiveness of the hydroxyl radical scavenger D-mannitol suggests that freely diffusible hydroxyl radicals do not make a significant contribution. This latter result is consistent with the majority of literature reports in which copper–peroxide-type complexes rather than hydroxyl radicals were found to be the principal reactive species involved in DNA cleavage by Cu(II)/Cu(I) redox cycling systems (59–61, 65). A mechanism consistent with the above photocleavage inhibition data is shown in Figure 6 (61). It is conceivable that Cu(II) bound to the pyridine linker of ligand **4** is photoreduced to Cu(I), which in turn reacts with hydrogen peroxide to produce a DNA-damaging Cu(I)-peroxide complex. Because the colorimetric BCS assay detected Cu(I) only when **4** was present, it can also be inferred that DNA photocleavage involves acridine-sensitized photo-reduction of Cu(II) to Cu(I).

DNA Photocleavage at Nucleotide Resolution. In order to map the sequence specificity of Cu(II)-assisted DNA photocleavage, pUC19 plasmid was linearized with *Eco*RI, 3'-end-labeled with [³⁵S]dATPαS, and then cut with *Fsp*I to produce a 138 bp restriction fragment (58). Reactions containing 15 μM bp of the radiolabeled DNA fragment in the absence and presence of 5 μM **4** and 5 μM CuCl₂ were irradiated at 419 nm for 2 h (20 mM sodium phosphate buffer pH 7.0). Half of the reactions were subsequently treated with 1.0% piperidine (90 °C, 30 min) in order to produce strand breaks at alkaline-labile lesions in the DNA. Products were electrophoresed adjacent to G, G + A, and T chemical sequencing reactions on a 10.0% denaturing polyacrylamide gel, after which, cleavage patterns were analyzed. Shown in Figure 7 are cleavage plots of a representative 40 bp sequence within the radiolabeled restriction fragment. The top 20 bases producing the highest levels of

**Figure 7.** Cleavage plots of a representative 40 bp DNA sequence. Photocleavage intensities as a function of DNA base were calculated by quantitating a storage-phosphor autoradiogram of DNA photocleavage products resolved on a 10.0% denaturing polyacrylamide gel (Figure S3 in Supporting Information). A total of 15 μM bp of ³⁵S 3'-end labeled 138 bp restriction fragment was irradiated at 419 nm in the presence of 5 μM **4** and 5 μM CuCl₂ without (A) and with (B) subsequent piperidine treatment. The ordinate is in units of *f_a* - *f_c*, where *f_a* is the fractional cleavage intensity produced in the photocleavage reaction and *f_c* is fractional cleavage intensity in a parallel control reaction in which DNA was irradiated in the absence of the Cu(II) complex of compound **4**, without (A) and with (B) the piperidine treatment. A horizontal line has been drawn through each plot in order to identify the top 20 DNA bases (inset) producing the highest levels of cleavage.

photocleavage appear in the inset of each plot. In the absence of piperidine, it is evident that the Cu(II) complex of **4** almost always produces frank strand breaks without a marked base preference (Figure 7A). This result suggests that photocleavage may involve hydrogen atom abstraction from deoxyribose. Because sugar residues are present in every nucleotide, reagents which function by hydrogen atom abstraction are expected to cleave at all nearby DNA sequences irrespective of base composition (11). Singlet oxygen and direct electron transfer from DNA nucleobases produce DNA damage predominately at guanine bases (11, 63) and are therefore unlikely to have made overriding contributions to the formation of frank strand breaks. Alternatively, the cleavage pattern was changed after the DNA photolysis reactions were treated with piperidine, showing preferential damage at guanine. This result indicates that alkaline-labile lesions were formed at guanine bases, either through the production of singlet oxygen and/or by direct electron transfer from DNA (Figure 7B).

CONCLUSION

In summary, our data indicate that Cu(II) markedly enhances DNA photocleavage by ligand **4** under near-physiological

conditions of temperature and pH. Although the precise cleavage mechanism is unknown, at this time we believe that the formation of frank strand breaks may involve acridine-sensitized photoreduction of Cu(II) to Cu(I) followed by reaction of 4/Cu(I) with hydrogen peroxide to form a copper–peroxide complex. Considering the bioavailability of copper at the cellular level, copper-based photonucleases are advantageous in comparison to complexes based on other metals or to chemical nucleases which require an external reducing agent for their activity. To the best of our knowledge, bis-acridine **4** is only the third example of a photonuclease that has been shown to cleave DNA by a process that involves direct photochemical reduction of copper (14, 15). Our future work will focus on mechanistic studies and on synthetic endeavors to develop new copper-based photonucleases for use in chemical and medical applications.

ACKNOWLEDGMENT

We thank Timothy C. Laeger, Prof. Marcus W. Germann, and Prof. W. David Wilson for their assistance (Georgia State University). Support of this research by the CAM-UAH (2005-012; A.L.), the CAM (GR-MAT 2004-0810; M.-M.R.), the National Science Foundation (CHE-9984772; K.B.G.), and the American Chemical Society Petroleum Research Fund (32897-G3; K.B.G.) is gratefully acknowledged.

Supporting Information Available: Table S1, the λ_{\max} values and extinction coefficients of nucleic acid samples used in competition dialysis experiments; Figure S1, ESI mass spectra of compound **4** and of 1:1 metallic complexes formed between compound **4** and Cu(II); Figure S2, concentration profile: percent photocleavage of pUC19 plasmid DNA in the absence and presence of 50 μ M to 2 μ M concentrations of CuCl₂ and/or compound **4**; Figure S3, storage-phosphor autoradiogram of a 10.0% denaturing polyacrylamide gel showing DNA photocleavage products at nucleotide resolution. This material is available free of charge via the Internet at <http://pubs.acs.org/BC>.

LITERATURE CITED

- (1) Barton, J. K. (1986) Metals and DNA: molecular left-handed complements. *Science* 233, 727–734.
- (2) Pyle, A. M., and Barton, J. K. (1990) Probing nucleic acids with transition metal complexes. *Prog. Inorg. Chem.* 38, 413–475.
- (3) Erkkila, K. E., Odom, D. T., and Barton, J. K. (1999) Recognition and reaction of metallointercalators with DNA. *Chem. Rev.* 99, 2777–2795.
- (4) Huber, P. W. (1993) Chemical nucleases: their use in studying RNA structure and RNA-protein interactions. *FASEB J.* 7, 1367–1375.
- (5) Pratviel, G., Bernadou, J., and Meunier, B. (1995) Carbon-hydrogen bond of DNA sugar units as targets for chemical nucleases and drugs. *Angew. Chem., Int. Ed. Engl.* 34, 746–769.
- (6) Burrows, C. J., and Muller, J. G. (1998) Oxidative nucleobase modifications leading to strand scission. *Chem. Rev.* 98, 1109–1151.
- (7) Pratviel, G., Bernadou, J., and Meunier, B. (1998) DNA and RNA cleavage by metal complexes. *Adv. Inorg. Chem.* 45, 251–312.
- (8) Cadet, J., and Vigny, P. (1990) The Photochemistry of Nucleic Acids. *Bioorganic Photochemistry* (Morrison, H., Ed.) Vol. 1, pp 1–272, Wiley, New York.
- (9) Kochevar, I. E., and Dunn, D. A. (1990) Photosensitized Reactions of DNA: Cleavage and Addition. *Bioorganic Photochemistry* (Morrison, H., Ed.) Vol. 1, pp 273–315, Wiley, New York.
- (10) Saito, I., and Nakatani, K. (1996) Design of DNA-cleaving agents. *Bull. Chem. Soc. Jpn.* 69, 3007–3019.
- (11) Armitage, B. (1998) Photocleavage of nucleic acids. *Chem. Rev.* 98, 1171–1200.
- (12) Barton, J. K., and Raphael, A. L. (1984) Photoactivated stereospecific cleavage of double-helical DNA by cobalt(III) complexes. *J. Am. Chem. Soc.* 106, 2466–2468.
- (13) Subramanian, R., and Meares, C. F. (1986) Photosensitization of cobalt bleomycin. *J. Am. Chem. Soc.* 108, 6427–6429.
- (14) Kuwahara, J., Suzuki, T., Funakoshi, K., and Sugiura, Y. (1986) Photosensitive DNA cleavage and phage inactivation by copper(II)-camptothecin. *Biochemistry* 25, 1216–1221.
- (15) Gude, L., Fernández, M. J., Grant, K. B., and Lorente, A. (2005) Syntheses and copper(II)-dependent DNA photocleavage by acridine and anthracene 1,10-phenanthroline conjugate systems. *Org. Biomol. Chem.* 3, 1856–1862.
- (16) Wilson, B., Gude, L., Fernández, M.-J., Lorente, A., and Grant, K. B. (2005) Tunable DNA photocleavage by an imidazole-acridine conjugate. *Inorg. Chem.* 44, 6159–6173.
- (17) Spector, W. S. (1956) *Handbook of Biological Data*, p 52, W. B. Saunders Company, Philadelphia.
- (18) Wacker, W. E. C., and Vallee, B. L. (1959) Nucleic acids and metals. I. Chromium, manganese, nickel, iron, and other metals in ribonucleic acid from diverse biological sources. *J. Biol. Chem.* 234, 3257–3262.
- (19) Cantor, K. P., and Hearst, J. E. (1966) Isolation and partial characterization of metaphase chromosomes of a mouse ascites tumor. *Proc. Natl. Acad. Sci. U.S.A.* 55, 642–649.
- (20) Bryan, S. E., Vizard, D. L., Beary, D. A., LaBiche, R. A., and Hardy, K. J. (1981) Partitioning of zinc and copper within subnuclear nucleoprotein particles. *Nucleic Acids Res.* 9, 5811–5823.
- (21) Fürst, P., and Hamer, D. (1989) Cooperative activation of a eukaryotic transcription factor: interaction between Cu(I) and yeast ACE1 protein. *Proc. Natl. Acad. Sci. U.S.A.* 86, 5267–5271.
- (22) Thiele, D. J. (1992) Metal-regulated transcription in eukaryotes. *Nucleic Acids Res.* 20, 1183–1191.
- (23) Mc Millin, D. R., and McNett, K. M. (1998) Photoprocesses of copper complexes that bind to DNA. *Chem. Rev.* 98, 1201–1219.
- (24) Eppley, H. J., Lato, S. M., Ellington, A. D., and Zaleski, J. M. (1999) Transition metal kinamycin model as a DNA photocleaver for hypoxic environments: bis(9-diazo-4,5-diazafluorene)copper(II) nitrate. *Chem. Commun.* 2405–2406.
- (25) Benites, P. J., Holmberg, R. C., Rawat, D. S., Kraft, B. J., Klein, L. J., Peters, D. G., Thorp, H. H., and Zaleski, J. M. (2003) Metal-ligand charge-transfer-promoted photoelectronic Bergman cyclization of copper metalloenediynes: photochemical DNA cleavage via C-4' H-atom abstraction. *J. Am. Chem. Soc.* 125, 6434–6446.
- (26) Dhar, S., and Chakravarty, A. R. (2003) Efficient visible light induced nuclease activity of a ternary mono-1,10-phenanthroline copper(II) complex containing 2-(methylthio)ethylsalicylaldehyde. *Inorg. Chem.* 42, 2483–2485.
- (27) Dhar, S., Senapati, D., Das, P. K., Chattopadhyay, P., Nethaji, M., and Chakravarty, A. R. (2003) Ternary copper complexes for photocleavage of DNA by red light: direct evidence for sulfur-to-copper charge transfer and d-d band involvement. *J. Am. Chem. Soc.* 125, 12118–12124.
- (28) Dhar, S., Senapati, D., Reddy, P. A., Das, P. K., and Chakravarty, A. R. (2003) Metal-assisted red light-induced efficient DNA cleavage by dipyrroquinoxaline-copper(II) complex. *Chem. Commun.* 2452–2453.
- (29) Vaidyanathan, V. G., and Nair, B. N. (2003) Oxidative cleavage of DNA by tridentate copper (II) complex. *J. Inorg. Biochem.* 93, 271–276.
- (30) Gupta, T., Dhar, S., Nethaji, M., and Chakravarty, A. R. (2004) Bis(dipyridophenazine)copper(II) complex as major groove directing synthetic hydrolase. *Dalton Trans.* 1896–1900.
- (31) Reddy, P. A., Santra, B. K., Nethaji, M., and Chakravarty, A. R. (2004) Metal-assisted light-induced DNA cleavage activity of 2-(methylthio)phenylsalicylaldehyde Schiff base copper(II) complexes having planar heterocyclic bases. *J. Inorg. Biochem.* 98, 377–386.
- (32) Dhar, S., and Chakravarty, A. R. (2005) Photosensitizer in a molecular bowl: steric protection enhancing the photonuclease activity of copper(II) scorpionates. *Inorg. Chem.* 44, 2582–2584.
- (33) Dhar, S., Nethaji, M., and Chakravarty, A. R. (2005) Effect of charge transfer bands on the photo-induced DNA cleavage activity of [1-(2-thiazolylazo)-2-naphtholato]copper(II) complexes. *J. Inorg. Biochem.* 99, 805–812.
- (34) Patra, A. K., Dhar, S., Nethaji, M., and Chakravarty, A. R. (2005) Metal-assisted red light-induced DNA cleavage by ternary L-methionine copper(II) complexes of planar heterocyclic bases. *Dalton Trans.* 896–902.

- (35) Patra, A. K., Nethaji, M., and Chakravarty, A. R. (2005) Red-light photosensitized cleavage of DNA by (L-lysine)(phenanthroline base)copper(II) complexes. *Dalton Trans.* 2798–2804.
- (36) Halliwell, B., and Gutteridge, J. M. C. (1984) Oxygen toxicity, oxygen radicals, transition metals and disease. *Biochem. J.* 219, 1–14.
- (37) Linder, M. C. (1991) *Biochemistry of Copper*, Plenum Press, New York.
- (38) Peña, M. M., Lee, J., and Thiele, D. J. (1999) A delicate balance: homeostatic control of copper uptake and distribution. *J. Nutr.* 129, 1251–1260.
- (39) Chevion, M. (1988) A site-specific mechanism for free radical induced biological damage: the essential role of redox-active transition metals. *Free Radical Biol. Med.* 5, 27–37.
- (40) Kady, I. O., and Tan, B. (1995) Metal-catalyzed intramolecular hydrolysis of phosphate esters. *Tetrahedron Lett.* 36, 4031–4034.
- (41) Lorente, A., Fernández-Saiz, M., Espinosa, J.-F., Jaime, C., Lehn, J.-M., and Vigneron, J.-P. (1995) Cyclo-bis-intercalands with acridine subunits linked by rigid spacers. *Tetrahedron Lett.* 36, 5261–5264.
- (42) Sambrook, J., Fritsch, E. F., and Maniatis, T. (1989) *Molecular Cloning: A Laboratory Manual*, 2nd ed., Cold Spring Harbor Laboratory, Cold Spring Harbor, NY.
- (43) Cohen, G., and Eisenberg, H. (1969) Viscosity and sedimentation study of sonicated DNA-proflavine complexes. *Biopolymers* 8, 45–55.
- (44) Ren, J., and Chaires, J. B. (2001) Rapid screening of structurally selective ligand binding to nucleic acids. *Methods Enzymol.* 340, 99–108.
- (45) Chaires, J. B. (2002) A competition dialysis assay for the study of structure-selective ligand binding to nucleic acids. *Current Protocols in Nucleic Acid Chemistry*, pp 8.8.1–8.3.8, John Wiley & Sons, New York.
- (46) Yang, X., and Grant, K. B. (2002) Chemical sequencing of restriction fragments 3'-end-labeled with [^{35}S]dATP α S. *J. Biochem. Biophys. Methods* 50, 123–128.
- (47) Couturier, Y., and Petitfaux, C. (1978) Composition and stability of copper complexes and pyridine amine-copper complexes. XI. Comparison of monopyridine mono- and diamines. *Bull. Soc. Chim. Fr.* 11–12, Pt. 1, 435–441.
- (48) Garcia Basallote, M., and Martell, A. E. (1988) New multidentate ligands. 29. Stabilities of metal complexes of the binucleating macrocyclic ligand BISBAMP and dioxygen affinity of its dinuclear cobalt(II) complex. *Inorg. Chem.* 27, 4219–4224.
- (49) Freifelder, D., Davison, P. F., and Geiduschek, E. P. (1961) Damage by visible light to the acridine orange–DNA complex. *Biophys. J.* 1, 389–400.
- (50) Piette, J., López, M., Calberg-Bacq, C. M., and Van, de Vorst, A. (1981) Mechanism for strand-break induction in DNA-proflavine complexes exposed to visible light. *Int. J. Radiat. Biol.* 40, 427–433.
- (51) Espinosa, J.-F., Fernández, M.-J., Grant, K. B., Gude, L., Rodrigo, M.-M., and Lorente, A. (2004) Synthesis, DNA intercalation and europium(III)-triggered DNA photocleavage by a bis-proflavine succinamide conjugate. *Tetrahedron Lett.* 45, 4017–4020.
- (52) Suh, D., and Chaires, J. B. (1995) Criteria for the mode of binding of DNA binding agents. *Bioorg. Med. Chem.* 3, 723–728.
- (53) Chaires, J. B., Leng, F., Przewloka, T., Fokt, I., Ling, Y.-H., Pérez-Soler, R., and Pribe, W. (1997) Structure-based design of a new bisintercalating anthracycline antibiotic. *J. Med. Chem.* 40, 261–266.
- (54) Pilch, D. S., Kirolos, M. A., Liu, X., Plum, G. E., and Breslauer, K. J. (1995) Berenil [1,3-bis(4'-amidinophenyl)triazene] binding to DNA duplexes and to a RNA duplex: evidence for both intercalative and minor groove binding properties. *Biochemistry* 34, 9962–9976.
- (55) Wilson, W. D., Tanious, F. A., and Fernández-Saiz, M. (1997) Evaluation of Drug-Nucleic Acid Interactions by Thermal Melting Curves. In *Drug-DNA Interaction Protocols* (K. R. Fox, Ed.) Humana Press, New Jersey.
- (56) Satyanarayana, S., Dabrowiak, J. C., and Chaires, J. B. (1993) Tris(phenanthroline)ruthenium(II) enantiomer interactions with DNA: mode and specificity of binding. *Biochemistry* 32, 2573–2584.
- (57) Oster, G. K., and Oster, G. (1959) Photoreduction of metal ions by visible light. *J. Am. Chem. Soc.* 81, 5543–5545.
- (58) Kellmann, A. (1974) Primary photochemical processes of cationic acridine orange in aqueous solution studied by flash photolysis. *Photochem. Photobiol.* 20, 103–108.
- (59) Yamamoto, K., and Kawanishi, S. (1989) Hydroxyl free radical is not the main active species in site-specific DNA damage induced by copper(II) ion and hydrogen peroxide. *J. Biol. Chem.* 264, 15435–15440.
- (60) Li, Y., and Trush, M. A. (1993) DNA damage resulting from the oxidation of hydroquinone by copper: role for a Cu(II)/Cu(I) redox cycle and reactive oxygen generation. *Carcinogenesis* 1303–1311.
- (61) Oikawa, S., and Kawanishi, S. (1998) Distinct mechanisms of site-specific DNA damage induced by endogenous reductants in the presence of iron(III) and copper(II). *Biochim. Biophys. Acta* 1399, 19–30.
- (62) Wong, A., Huang, H.-C., and Crooke, S. T. (1984) Mechanism of deoxyribonucleic acid breakage induced by 4'-(9-acridinylamino)-methanesulfon-m-anisidide and copper: role for cuprous ion and oxygen free radicals. *Biochemistry* 23, 2946–2952.
- (63) Devasagayam, T. P., Steenken, S., Obendorf, M. S., Schulz, W. A., and Sies, H. (1991) Formation of 8-hydroxy(deoxy)guanosine and generation of strand breaks at guanine residues in DNA by singlet oxygen. *Biochemistry* 30, 6283–6289.
- (64) Di Mascio, P., Wefers, H., Do-Thi, H. P., Lafleur, M. V., and Sies, H. (1989) Singlet molecular oxygen causes loss of biological activity in plasmid and bacteriophage DNA and induces single-strand breaks. *Biochim. Biophys. Acta* 1007, 151–157.
- (65) Masarwa, M., Cohen, H., Meyerstein, D., Hickman, D. L., Bakac, A., and Espenson, J. H. (1988) Reactions of low-valent transition-metal complexes with hydrogen peroxide. Are they "Fenton-like" or not? 1. The case of Cu $^{+}$ aq and Cr $^{2+}$ aq. *J. Am. Chem. Soc.* 110, 4293–4297.

BC0601828